

Characterisation of Stress Intensity Factor with Magnetic Flux Signal Leakage in Stable Fatigue Crack Growth Region

S. R. Ahmad, A. Arifin*, S. Abdullah, M. F. M. Yunoh
Department of Mechanical and Materials Engineering,
Faculty of Engineering and Built Environment,
Universiti Kebangsaan Malaysia,
43600 UKM Bangi, Selangor, Malaysia

*azli@ukm.edu.my

ABSTRACT

This paper presents the characterisation of the stress intensity factor range ΔK , with the magnetic flux gradient, $dH(y)/dx$ signals obtained using the metal magnetic memory (MMM) method during fatigue crack growth test. The MMM method is a passive non-destructive testing technique developed for the examination of self-magnetic leakage field signals which were generated in the stress concentration zones. In this paper, the fatigue crack growth test was conducted by applying a constant amplitude loading at different stress ratios. The scanning device and crack opening displacement gauges were used for acquiring the magnetic signals and crack growth parameter, respectively. The relationship between the $dH(y)/dx$ signals, fatigue crack growth rate, da/dN and ΔK was determined. As a result, some similarities were observed between the ΔK and $dH(y)/dx$ signals; wherein both were seen to increase with an increase in the value of da/dN . Furthermore, the analysis of the relationship between $dH(y)/dx$ and ΔK focused on the stable crack growth region and noted that the correlation of determination ranged between 0.9286 - 0.9788. This indicates that $dH(y)/dx$ signals can be used to evaluate the fatigue crack growth of the material.

Keywords: Crack, fatigue, magnetic flux, steel, stress intensity factor

Introduction

The primary concern about failure of various engineering components such as in automobile industries is due to fatigue damage. This is because, during the service, these components experienced cyclic loading [1]. Fatigue failure process normally consists of three regions, that is: fatigue cracks initiation, a stable fatigue crack growth, and the final fracture [2]. Out of these three regions, significant efforts have been made to study the stable crack growth region since this fatigue stage occupies a major portion of the material's fatigue life. This region is very important for determining the remaining life of engineering materials [3]. Fracture mechanics approach deals with fracture phenomena which combines the mechanics of cracked bodies and mechanical properties. Through this concept, the parameter of stress intensity factor, K is used to assess the strength of a substance. When the K value reaches a certain critical value depending on the fracture toughness value of the material, the failure occurs [4]. The fatigue crack growth behaviour can be described by the relationship between fatigue crack growth rate, da/dN and stress intensity factor range, ΔK . The straight line obtained in the middle region on the log-log plot represented by the Paris Law equation [5].

Failure to detect defects as early as possible can lead to an increased risk of major accidents. This occurs with a gradual growth of the initial defect, leading to the fracture of the material. The commonly used technique for determining the functioning or the status of the component is through checking for defects using the non-destructive testing (NDT) method [6]. The stress concentration area is an important element which must be analysed as it is the major source of growth of the defects or damages. Along with technological developments in the NDT, the metal magnetic memory (MMM) method was introduced for the detection of stress concentration zones [7]. In comparison with other NDT methods, the MMM method can diagnose early damages and developing defects in the material. In addition, this method is easy to use, has a high sensibility, and is cost and time effective [8].

The MMM method is based on measuring the self-magnetization leakage field and can be used for detecting the development of fatigue crack [9]. The changes in the normal component, $H(y)$ signals and the tangential component, $H(x)$ signals have been investigated by Wang et al [10] when evaluating the fatigue damage of 0.45% C steel specimens during the tension-compression cyclic test. Huang et al [11] studied the effect of the $H(y)$ signals and the magnetic flux gradient signals, $dH(y)/dx$ on the surface of ferromagnetic structural steel throughout the dynamic three-point bending fatigue tests. Chong et al [8] analysed the distribution and variation of the MMM signals during fatigue crack propagation. It shows that the magnetic parameters increased with the increase of fatigue crack length, therefore the

MMM signals was possible to evaluate the fatigue damage of the ferromagnetic components.

From the previous studies, it can be identified that the signals from MMM method are capable of detecting the stress concentration zone and evaluating the fatigue failure. However, till date, the MMM method is still lack of the physical models and quantitative criteria for the detection of defects, further researches are necessary to attain a better understanding of this method and to find better correlation especially between MMM and fatigue [12]. This study aims to characterise the magnetic flux gradient signals, $dH(y)/dx$ parameter obtained through the MMM method with the fatigue crack growth parameter that is stress intensity factor range, ΔK . In this study, fatigue crack growth test of ferromagnetic steel was conducted by using different stress ratio. Fatigue crack growth behaviour in stable region explained by the Paris Law equation. Furthermore, the magnetic flux detection during the fatigue test was carried out using the MMM method. The relation between the $dH(y)/dx$ signals and the fatigue crack growth parameter was characterised. The fatigue crack growth in stable crack propagation region explained by using $dH(y)/dx$ signals and the relation between $dH(y)/dx$ signals and ΔK discussed. Through this study, it presumes that the $dH(y)/dx$ signals value can will increase during the fatigue crack growth process and the $dH(y)/dx$ signals has the potential to replace ΔK parameter in describing fatigue crack growth behaviour in stable region.

Methodology

The The material used in this study was a ferromagnetic material SAE 1045 medium carbon steel which is commonly used in most engineering and construction works [6]. The tensile tests were conducted to obtain the monotonic properties of the material. The specimens were designed according to the ASTM:8M-11 standard. Thereafter, the constant amplitude loading fatigue test was performed using a 100 kN Servo-Hydraulic Machine. Three stress ratio, R values were applied in the test. The test condition was selected to observe the stable crack propagation during the magnetic flux monitoring process. From our previous study, it has been found that a maximum load of more than 7 kN can lead to an unstable crack growth. Table 1 described the loading design used in this study.

Table 1: Loading conditions of the fatigue test

Frequency (Hz)	10		
Stress ratio, R	0.1	0.2	0.3
Maximum load, P_{max} (kN)	4.44	5.00	5.71
Minimum load, P_{min} (kN)	0.44	1.00	1.71

The fatigue crack growth test specimens were designed according to the ASTM E647 standard. Figure 1 shows the schematic geometry of the specimen. This specimen is also referred to as an eccentrically-edge crack loaded single tension specimen. According to the standard, the initial crack was in the middle of the specimen with a length of 22 mm. The crack opening displacement (COD) device was used to measure the fatigue crack growth parameter, which is the propagation of the crack length on the specimen, and the range of the stress intensity factor, ΔK . The set-up of the fatigue crack growth experiment is shown in Figure 2.

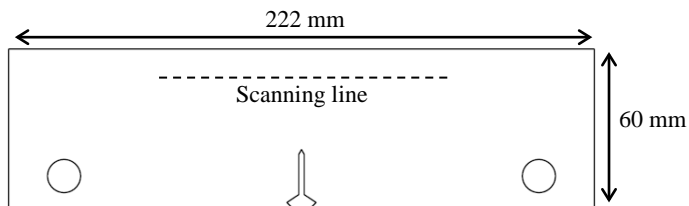


Figure 1: Schematic geometry of fatigue crack growth specimen

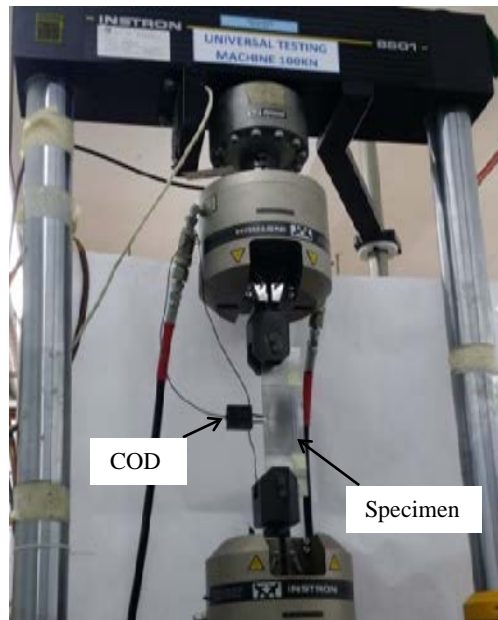


Figure 2: The Servo-Hydraulic Machine with the specimen and COD attached

During the cyclic test, for every 1 mm crack length propagation, the fatigue test was halted for the measurement of the magnetic signals. The magnetic signals were captured using the MMM scanning device shown in Figure 3. Meanwhile, Figure 4 shows the method used to attach the MMM sensor to the specimen. The MMM sensor was rolled on the 100-mm scanning line length. The magnetic signals were captured by using sensors 1 and 2. The distance between the wheel and sensor 1 was 5 mm, while the distance between the wheel and sensor 2 was 25 mm. The cyclic test was conducted till the occurrence of a final failure of the specimen. The whole process was repeated for the other load conditions. Subsequently, the magnetic signals were analysed by using the MMM software.

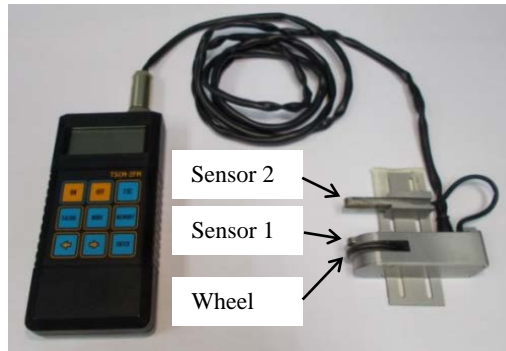


Figure 3: The MMM scanning device

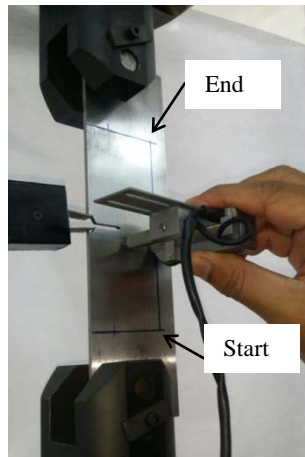


Figure 4: The MMM sensor rolled through the scanning line on the specimen

Fatigue crack growth equation

The logarithmic plot of da/dN and ΔK shows that the complete fatigue life and the fatigue regions were separated by the ΔK value. The value of the stress intensity reflected the severity of the cracks. Region I was located below the fatigue crack growth threshold ΔK_{th} value. In this region, the crack growth did not generally occur and the crack growth rate was at the lowest. Region II was seen to correspond to the stable macroscopic crack growth as displayed by a straight line in the log–log plot [13]. The relationship of the da/dN and ΔK in the stable crack growth region can be written based on the Paris law as shown in Equation (1)

$$da/dN = C(\Delta K)^m, \Delta K_{th} < \Delta K < K_{Ic} \quad (1)$$

where ΔK_{th} is the fatigue threshold, and K_{Ic} is the fracture toughness of the material. C and m are material constant values. Region III is the final failure region where the crack growth rates were the highest [13].

Results and Discussion

Material properties determination

The monotonic properties of the SAE 1045 medium carbon steel were obtained using the tensile test as shown in Table 2. The yield and ultimate tensile strengths obtained in this experiment were compared to the same type of material used in previous studies [14]. It was found that the percentage difference between the experimental values and the reference values was 5 % for the yield strength value and 12 % for the ultimate tensile strength value. Therefore, the monotonic properties value can be accepted. In addition, the crack growth coefficient, crack growth exponent, threshold, and fracture toughness was obtained from a previous study reported by Pugno et al [14] as shown in Table 3. These values were important and used for subsequent fatigue crack growth analysis.

Table 2: Material properties of SAE 1045 steel from tension test

Properties	Tension test
Yield strength (MPa)	363.5
Ultimate tensile strength (MPa)	709.6
Modulus Young (GPa)	206.7

Table 3: Fatigue crack growth properties of SAE 1045

Crack growth coefficient (m/cycle)	Crack growth exponent	Threshold (MPa√m)	Fracture toughness (MPa√m)
8.20E-13	3.5	7.1	80

Fatigue crack growth behaviour

Figure 4 presents the results obtained by the fatigue test which shows an increase in the crack length due to the application of a number of cycles for every test condition. The crack growth rate, da/dN was obtained from the slope of the curve. As shown in the figure, the number of cycles at failure for $R = 0.1, 0.2,$ and 0.3 were 68,025, 66,038, and 60,936 cycles, respectively.

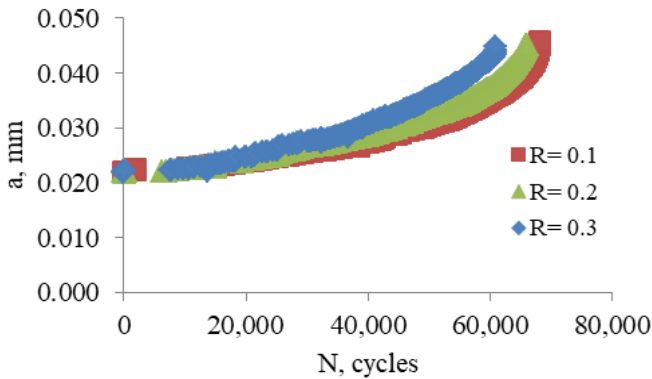


Figure 4: Crack length versus the number of cycles for each R value

The results shows that the fracture life for $R = 0.3$ was shorter than $R = 0.2$ and 0.1 . As stated in Table 1, the maximum loading for $R = 0.3$ was higher than $R = 0.2$ and 0.1 . This shows that the stress ratio could cause an increase in the maximum load. The number of cycles to failure were seen to be dependent on the magnitude of the stress applied. Therefore, with an increase in the stress ratio, there was an increase in the crack growth rate and a decrease in the fracture life [15].

Figure 5 presents the log-log plot for da/dN and ΔK which describes the fatigue crack growth behaviour for every stress ratio. The figure shows that the resultant sigmoidal curve was divided into 3 regions. This study primarily focused on Region 2 which represented the stable crack propagation region. The determination of Region I and Region II was based

on the threshold values obtained from an earlier study [3] as shown in Table 3. The properties for fatigue crack growth are shown for $R = 0$.

From the experiments, the minimum stress intensity factor range values for $R = 0.1, 0.2,$ and 0.3 were $27.64, 26.74,$ and $27.16 \text{ MPa}\sqrt{\text{m}}$, respectively. According to previous studies, however, the threshold value for this material is $7.1 \text{ MPa}\sqrt{\text{m}}$. This is because the recommended testing process for obtaining the complete range of the sigmoidal curve is to perform the constant amplitude test and ΔK -decreasing test. The ΔK -decreasing test was used for generating the fatigue crack growth data from Region I to the middle of the stable crack growth region. Meanwhile, the constant amplitude test was performed to acquire the fatigue crack growth data from the middle of Region II to Region III [16]. In this study, the only test conducted was the constant amplitude test. The determination of Region II and Region III was based on the fracture toughness of the material. Referring to the experimental results, when the value of ΔK exceeds the fracture toughness value at $80 \text{ MPa}\sqrt{\text{m}}$, the da/dN value rapidly increased. The final value of ΔK recorded by the COD device was $102.39 \text{ MPa}\sqrt{\text{m}}$ for $R = 0.1$, $98.07 \text{ MPa}\sqrt{\text{m}}$ for $R = 0.2$ and $85.04 \text{ MPa}\sqrt{\text{m}}$ for $R = 0.3$.

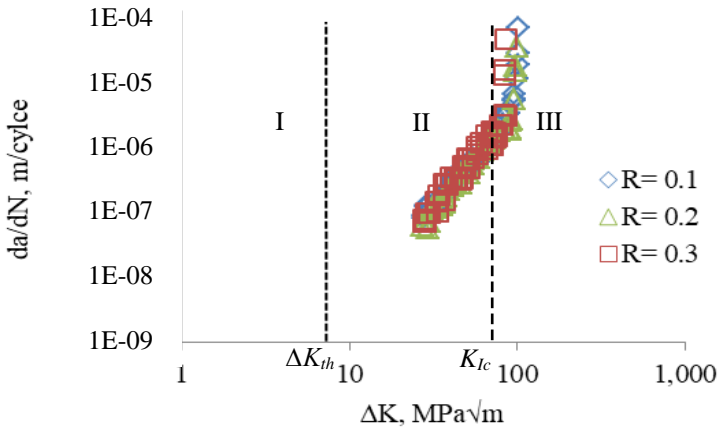


Figure 5: Fatigue crack growth behaviour for each value of R

The values of C and m were determined from the steady crack growth region based on the Paris law equation described in Figure 6. The values of da/dN and ΔK were taken at the crack length of 1 mm to 18 mm , determined as Region II. For the three curves, the crack growth exponent values were the same at 3.5 . Although the test was conducted at different stress ratios, the crack growth exponent value was still the same as it

represented the material constant [13]. The crack growth coefficient was the intercept value of the log da/dN axis. Figure 6 shows that the crack growth coefficient value for $R = 0.1, 0.2$ and 0.3 were $8.444E^{-13}$, $8.773E^{-13}$, and $9.830E^{-13}$, respectively. Although no big difference was observed noted between the curves from the figure, the obtained crack growth coefficient values indicated a difference in the crack growth rate. With the increase of stress ratio value, the fatigue crack growth rate, da/dN will also increase [15].

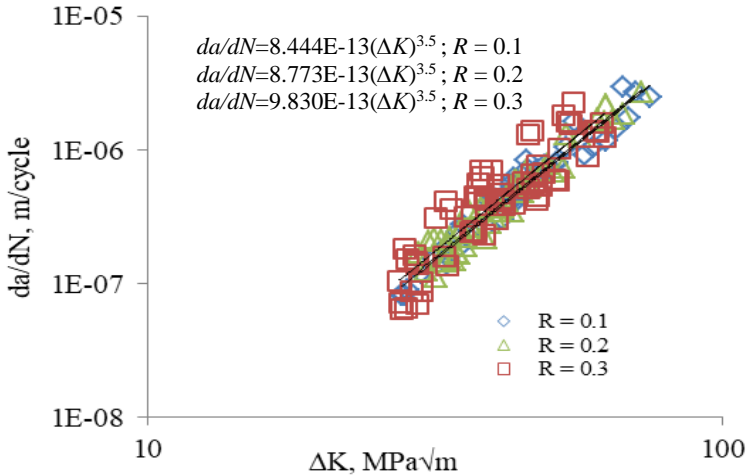
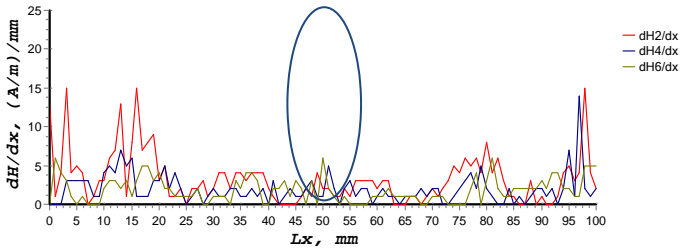


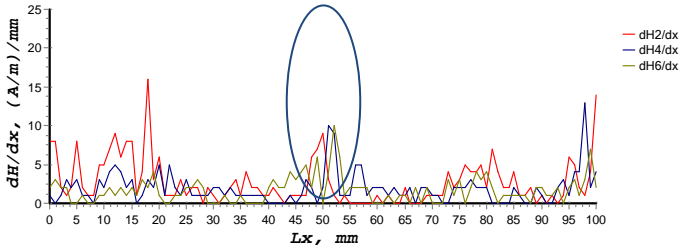
Figure 6: Determination of fatigue crack growth coefficient

Analysis of the stress concentration zone

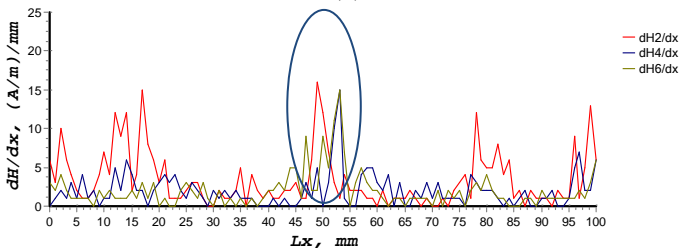
The magnetic signals were obtained via two sensors. Nevertheless, from the analysis, it was seen that Sensor 2 provided better signals in comparison to Sensor 1. This was due to the difference in the distance of the sensors from the initial crack length. Sensor 1 was less sensitive due to a larger distance from the initial crack length when compared to sensor 2 [10]. Accordingly, the analysis of the stress concentration zone in this study was based on the signals from Sensor 2. The MMM scanning device used in this study detects the normal component signals, $H(y)$ and the magnetic flux gradient signals, $dH(y)/dx$. However, only the $dH(y)/dx$ signals have been presented because the MMM gradient signals were more sensitive to the degree of damage in comparison to the $H(y)$ signals [17].



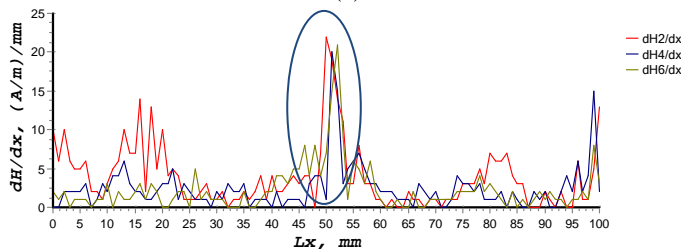
(a)



(b)



(c)



(d)

Figure 7: Magnetic signal trends for $R = 0.1$ ($dH2/dx$), $R = 0.2$ ($dH4/dx$) & $R = 0.3$ ($dH6/dx$) on the crack length of: (a) 4 mm, (b) 8 mm, (c) 12 mm, (d) 16 mm

Figure 7 shows the variation of $dH(y)/dx$ signals along the scanning line. The y-axis was the $dH(y)/dx$ signal values whereas the x-axis was the scanning line distance (100 mm). When taking the magnetic signals, the sensor was moved over the scanning line and the MMM signal was taken at each crack length extension of 1 mm. Nevertheless, as a summary in Figure 7, the authors only shows the changes in magnetic signals obtained on the crack length of 4 mm, 8 mm, 12 mm and 16 mm only for each stress ratio value. It was observed that there were significant changes in the $dH(y)/dx$ signals for a scanning distance of 45 - 55 mm. The changes in the $dH(y)/dx$ values within these regions were as expected as the specimen notch was present in this area [9]. The stress was mainly concentrated in the areas with notches; therefore, the crack growth of originates here.

Based on the results, there was an increase in the $dH(y)/dx$ values as the crack length increases. A similar change in the $dH(y)/dx$ signals was noted for all the three R values. This shows that the $dH(y)/dx$ signal values can be used for detecting the stress concentration zone. The effect of stress on the ferromagnetic material can result in spontaneous magnetic signals, which can probably be applied for evaluating the degree of damage [16]. The ferromagnetic theory shows that the magnetization was irreversible. When the load was removed, there was an increase in the specimen's magnetic permeability, and which could not revert to its original value. There was an increase in the specimen's magnetism due to the loading cycle which is associated with the load magnitude [18].

Based on Figure 7, although the $dH(y)/dx$ signals were correlated to the fatigue crack growth process, some other $dH(y)/dx$ signals were also being detected by the MMM scanning device sensors at a scanning distance of 0 – 25 mm and 75 – 100 mm, as shown in Figures 7(a) – 7(d). However, these signals were not analysed in our study because no significant changes were noted. These signals were detected by the sensor based on the effects of the initial magnetic field from the fatigue testing machine clamps and environmental magnetic field [17,19].

Relations of crack growth parameter and magnetic parameter

It was observed from the analysis of the fatigue crack growth behaviour that the crack length within the stable crack propagation region ranged between 1 - 18 mm. Therefore, $dH(y)/dx$ values at the crack length of 1 – 18 mm for each stress ratio value were shown in Table 4.

Table 4: Changes in the magnetic signals by the elongation of the crack

Crack length (mm)	$dH(y)/dx$ value		
	$R = 0.1$	$R = 0.2$	$R = 0.3$
1	2	2	3
2	3	3	3
3	3	4	4
4	4	5	6
5	5	6	7
6	7	7	8
7	8	8	9
8	9	10	10
9	10	11	10
10	12	13	11
11	15	14	14
12	16	15	15
13	18	17	16
14	19	18	18
15	20	19	19
16	22	20	21
17	28	23	29
18	32	26	34

In Figure 8, the relation between the $\log da/dN$ and the $\log dH(y)/dx$ within the stable crack growth regions was observed. Generally, it was observed that for the three values of R , there was an increase in the $dH(y)/dx$ value with increasing values of da/dN [20]. The graph of da/dN against $dH(y)/dx$ in Figure 8 shows a similar pattern as seen in the graph of da/dn against ΔK in Figure 6, especially for the stable crack growth region. It was noted that the coefficient of determination R^2 for the three R values ranged between 0.9405 - 0.9746. Since the R^2 valued is closed to 1, this shows that the fatigue crack growth behaviour could be explained based on the magnetic parameters.

In a study by Dubov [9], the MMM methodology can be used to identify the stress concentration zones. Based on the concept of fracture mechanics, the stress intensity factor range parameter is being used in the analysis of fatigue crack growth. The ability of the MMM signals to replace the values of ΔK for analysing the fatigue cracks can be determined based on the graph of $\log dH(y)/dx$ versus $\log \Delta K$, as described in Figure 9. It was noted that the coefficient of determination R^2 obtained for the three R values ranged between 0.9286 - 0.9788. The results shows that the relation between the $dH(y)/dx$ signals and the ΔK was acceptable. Hence, the $dH(y)/dx$ signals

can be proposed as an alternative for replacing ΔK when analysing fatigue crack growth.

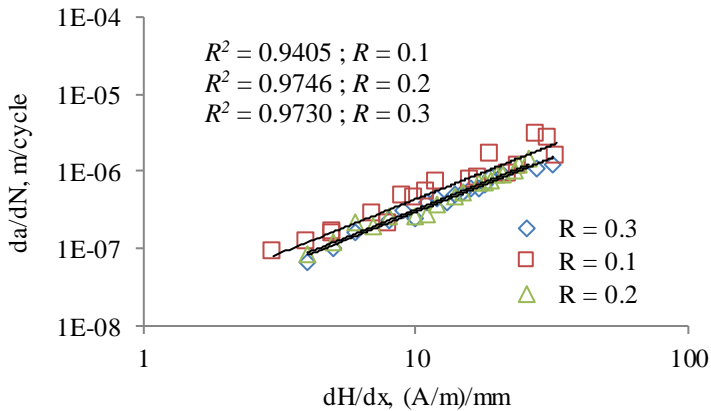


Figure 8: Relationship of da/dN versus $dH(y)/dx$ in second region of fatigue crack growth

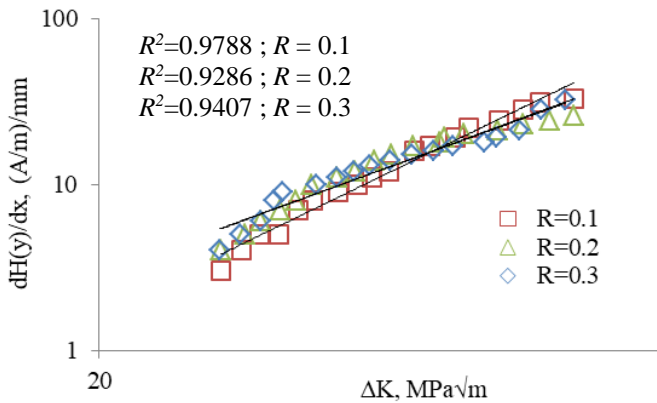


Figure 9: Relationship between $dH(y)/dx$ signals and ΔK

Conclusion

In this study, the fatigue crack growth behaviour of SAE 1045 medium carbon steel was studied using the MMM method. The crack growth

parameter was characterised by the magnetic flux gradient, $dH(y)/dx$ signals obtained from the MMM method. As the result, the stress concentration zone of the specimens can be detected and analysed by the MMM signals. For each value of R , the values of the $dH(y)/dx$ signals increased with increasing values of da/dN . The relationship between the $dH(y)/dx$ and ΔK was established with the correlation of determination R^2 obtained were between 0.9286 - 0.9788. It is concluded that the $dH(y)/dx$ signals can serve as an alternative parameter for analysing the fatigue crack growth within the stable region.

Acknowledgement

The authors would like to express their gratitude to Universiti Kebangsaan Malaysia and Ministry of Education Malaysia for funding under the grant of FRGS/2/2014/TK01/UKM/02/03 for supporting this project research.

References

- [1] M. Okayasu & H. Fukui, "Effects of Cyclic Loading on Fatigue Properties of Austenite Stainless Steel," *Journal of Mechanical Science and Technology* 29(9): 3663–3668 (2015).
- [2] X. Wang, D. Yin, F. Xu, B. Qiu, and Z. Gao, "Fatigue crack initiation and growth of 16MnR steel with stress ratio effects," *Int. J. Fatigue* 35 (1), 10–15 (2012).
- [3] H. Xing, R. Wang, M. Xu, and J. Zhang, "Correlation between Crack Growth Rate and Magnetic Memory Signal of X45 Steel," *Key Engineering Materials* 358, 2293–2296 (2007).
- [4] A. S. Ribeiro, A. L. L. Silva, M. P. Abilio, "Evolution of Fatigue History," 21st Brazilian Congress of Mechanical (2011).
- [5] M. L. Zhu, F. Z. Xuan & S. T. Tu, "Effect of Load Ratio on Fatigue Crack Growth in the Near-Threshold Regime: A Literature Review, and a Combined Crack Closure and Driving Force Approach," *Engineering Fracture Mechanics* 141, 57–77 (2015).
- [6] V. L. de A. Freitas, V. H. C. de Albuquerque, E. de M. Silva, A. A. Silva, and J. M. R. S. Tavares, "Nondestructive Characterization of Microstructures and Determination of Elastic Properties in Plain Carbon Steel using Ultrasonic Measurements," *J. Chem. Inf. Model.* 53 (9), 1689–1699 (2013).
- [7] Z. D. Wang, K. Yao, B. Deng, and K. Q. Ding, "Quantitative study of metal magnetic memory signal versus local stress concentration," *NDT E Int.* 43 (6), 513–518 (2010).

- [8] L. Chongchong, D. Lihong, W. Haidou, L. Guolu, and X. Binshi, "Metal magnetic memory technique used to predict the fatigue crack propagation behavior of 0.45%C steel," *J. Magn. Magn. Mater.* 405, 150–157 (2016).
- [9] A. A. Dubov, "Development of a Metal Magnetic Memory Method," *Chem. Pet. Eng.* 47 (12) 28–29 (2012).
- [10] H. P. Wang, L. H. Dong, S. Y. Dong, B. S. Xu, W. Hui-peng, D. Lihong, D. Shi-yun, and X. U. Bin-shi, "Fatigue damage evaluation by metal magnetic memory testing," *J. Cent. South Univ.* 21 (1), 65–70 (2014).
- [11] H. Huang, S. Jiang, R. Liu, and Z. Liu, "Investigation of Magnetic Memory Signals Induced by Dynamic Bending Load in Fatigue Crack Propagation Process of Structural Steel," *J. Nondestruct. Eval.* 33, 407–412 (2014).
- [12] Arifin, A., Jusoh, W. Z. W., Abdullah, S., Jamaluddin, N. & Ariffin, A. K. "Investigating the Fatigue Failure Characteristics of A283 Grade C Steel Using Magnetic Flux Detection," *Steel and Composite Structures* 3, 601–614 (2015).
- [13] C. A. R. P. Baptista, A. M. L. Adib, M. A. S. Torres, and V. A. Pastoukhov, "Describing fatigue crack growth and load ratio effects in Al 2524 T3 alloy with an enhanced exponential model," *Mech. Mater.* 51, 66–73 (2012).
- [14] N. Pugno, M. Ciavarella, P. Cornetti, and A. Carpinteri, "A generalized Paris law for fatigue crack growth," *J. Mech. Phys. Solids* 54 (7), 1333–1349 (2006).
- [15] F. S. Silva, "The importance of compressive stresses on fatigue crack propagation rate," *Int. J. Fatigue* 27 (10–12), 1441–1452 (2005).
- [16] S. Changliang, D. Shiyun, X. Binshi, and H. Peng, "Stress concentration degree affects spontaneous magnetic signals of ferromagnetic steel under dynamic tension load," *NDT E Int.* 43 (1) 8–12 (2010).
- [17] H. Xing, Y. Dang, B. Wang, and J. Leng, "Quantitative metal magnetic memory reliability modeling for welded joints," *Chinese J. Mech. Eng.* 29 (2), 372–377 (2016).
- [18] X. Jian, X. Jian, and G. Deng, "Experiment on relationship between the magnetic gradient of low-carbon steel and its stress," *J. Magn. Magn. Mater.* 321 (21) 3600–3606 (2009).
- [19] J. Leng, M. Xu, S. Zhao, and J. Zhang, "Fatigue damage evaluation on ferromagnetic materials using magnetic memory method," in *International Conference on Measuring Technology and Mechatronics Automation, ICMTMA'09* 784–786 (2009).
- [20] H. Huang, S. Jiang, Y. Wang, L. Zhang, and Z. Liu, "Characterization of Spontaneous Magnetic Signals Induced by Cyclic Tensile Stress in Crack Propagation Stage," *J. Magn. Magn. Mater.*, 365, 70–75 (2014).